

Supporting Information

Heterogeneous activation of peroxymonosulfate by stable Co-MOF for efficient degradation of organic dye pollutant

Wei Xie,^a Yuan Yuan,^a Wei Jiang,^a Shu-Ran Zhang,^a Guang-Juan Xu,^a Yan-Hong Xu,
^{*a}, and Zhong-Min Su^{*b}

*^a Key Laboratory of Preparation and Applications of Environmental Friendly
Materials (Jilin Normal University), Ministry of Education, Changchun 130103, Jilin,
PR China*

*^b Institute of Functional Material Chemistry, Faculty of Chemistry, Northeast Normal
University, Changchun 130024, Jilin (P. R. China)*

** Corresponding author*

E-mail: xuyh198@163.com; zmsu@nenu.edu.cn

S1. Materials and Methods

All chemical reagents for synthesis were purchased commercially and were used directly without further purification. Powder X-ray diffraction (PXRD) data were obtained on a Rigaku model RINT Ultima III diffractometer by depositing powder on glass substrate, from $2\theta = 3^\circ$ up to 50° with 0.02° increment. The IR spectrum was measured with a Perkin-elmer model FT-IR-frontier infrared spectrometer. Thermogravimetric analysis (TGA) was recorded on a Q5000IR analyser (TA Instruments) with an automated vertical overhead thermobalance heated from room temperature to 700°C with a heating rate of $5^\circ\text{C}/\text{min}$ under nitrogen gas atmosphere. Elemental analyses (C, H and N) were conducted on a Perkin-Elmer 240C elemental analyzer. X-ray photoelectron spectra (XPS) were recorded on an ESCALAB250Xi electron spectrometer (Thermo Fisher Scientific Inc., Waltham, MA, USA). The UV-vis absorption spectra were carried out using Jasco V-770 spectrometer (JAPAN) spectrophotometer. The metal ion content in the solution is tested by ICP mass spectrometer (NexION 350X, United States). Total organic carbon was analyzed with a TOC analyzer (Shimadzu TOC-L-CPH).

S2. Synthesis of Co-MOF

$\text{Co}(\text{NO}_3)_2 \cdot 6\text{H}_2\text{O}$ (0.058 g, 0.2 mmol), 4-(pyridin-4-yl) benzoic acid (HPBA, 0.020 g, 0.1 mmol), and 2-picolinic acid (Hpic, 0.024 g, 0.2 mmol) were dissolved in a 6 mL mixture of N,N-dimethylacetamide (DMA) and H_2O (v/v = 1:1). The clear solution was sealed in a 10 mL Teflon-lined stainless vessel and heated at 110°C for 72 h. The vessel was then cooled slowly down to the room temperature. Reddish-brown block crystals of Co-MOF were separated in 76% yield based on HPBA ligand. Elemental microanalysis for $\text{C}_{20}\text{H}_{20.5}\text{N}_{2.5}\text{O}_{6.5}\text{Co}$, calculated (%): C, 52.36; H, 4.50; N, 7.63. Found (%): C, 52.67; H, 4.79; N, 7.52. IR data (KBr cm^{-1}): 3254 (m), 3068 (m), 2928 (m), 2691 (w), 2151 (w), 1977 (w), 1659 (s), 1610 (s), 1564 (s), 1396 (s), 1179 (m), 1008 (s), 838 (s), 787 (s), 660 (w), 562 (w), 490 (m).

S3. Single-crystal X-ray diffraction

The X-ray single crystal data diffraction data of the Co-MOF was collected at 293 K on a Bruker APEXII CCD diffractometer with graphite-monochromated Mo K α radiation ($\lambda = 0.71069 \text{ \AA}$). Absorption corrections were applied using multi-scan technique. The structure was solved by Direct Method and refined by full-matrix least-squares techniques using the SHELXL-2018 program¹ within WINGX software². Non-hydrogen atoms were refined with anisotropic temperature parameters. All the solvent molecules which are highly disordered and not able to be modeled were treated by the SQUEEZE³ routine in PLATON⁴. The detailed crystallographic data and structure refinement parameters for Co-MOF (CCDC: 2176542) are summarized in Table S1. Selected bond lengths (\AA) and angles ($^\circ$) for Co-MOF are given in Table S2.

Table S1 Crystal data and structure refinements for Co-MOF.

Identification code	Co-MOF
formula	[Co(PBA)(pic)(H ₂ O)]·H ₂ O·0.5DMA
Formula weight	458.82
Crystal system	Monoclinic
Space group	<i>P2₁/c</i>
<i>a</i> (\AA)	13.584 (2)
<i>b</i> (\AA)	9.6137 (12)
<i>c</i> (\AA)	15.958 (2)
α ($^\circ$)	90.000
β ($^\circ$)	106.260 (5)
γ ($^\circ$)	90.000
<i>V</i> (\AA^3)	2000.6 (5)
<i>Z</i>	4
<i>D</i> _{calcd.} [g cm ⁻³]	1.312
<i>F</i> (000)	804
Reflections collected / unique	19654 / 3527
<i>R</i> (int)	0.0902
Goodness-of-fit on <i>F</i> ²	1.054
<i>R</i> ₁ ^a [<i>I</i> > 2 σ (<i>I</i>)]	0.0513
<i>wR</i> ₂ ^b (all data)	0.1422

^a $R_1 = \frac{\sum ||F_o| - |F_c||}{\sum |F_o|}$, ^b $wR_2 = \frac{|\sum w(|F_o|^2 - |F_c|^2)|}{\sum w(F_o^2)^2}^{1/2}$.

Table S2 Selected bond lengths (Å) and angles (°) for Co-MOF.

Co-MOF			
Co(1)-O(1)	2.056(2)	Co(1)-O(3)	2.102(3)
Co(1)-O(2)#1	2.105(2)	Co(1)-O(5)	2.131(2)
Co(1)-N(1)	2.142(3)	Co(1)-N(2)#2	2.173(3)
O(1)-Co(1)-O(3)	90.49(10)	O(1)-Co(1)-O(2)#1	89.19(9)
O(3)-Co(1)-O(2)#1	92.07(10)	O(1)-Co(1)-O(5)	171.55(9)
O(3)-Co(1)-O(5)	91.58(9)	O(2)#1-Co(1)-O(5)	98.92(9)
O(1)-Co(1)-N(1)	78.03(10)	O(3)-Co(1)-N1	90.13(11)
O(2)#1-Co(1)-N1	167.05(10)	O(5)-Co(1)-N1	93.77(9)
O1-Co(1)-N(2)#2	90.19(10)	O(3)-Co(1)-N(2)#2	177.31(10)
O(2)#1-Co(1)-N(2)#2	85.33(10)	O(5)-Co(1)-N(2)#2	88.11(9)
N(1)-Co(1)-N(2)#2	92.56(11)	C(1)-O(2)-Co(1)#3	123.9(2)
C(1)-O(1)-Co(1)	117.9(2)	C(7)-O(3)-Co(1)	126.4(2)
C(16)-N(2)-Co(1)#4	123.1(2)	C(17)-N(2)-Co(1)#4	120.5(2)
C(6)-N(1)-Co(1)	129.5(2)	C(2)-N(1)-Co(1)	112.5(2)

Symmetry transformations used to generate equivalent atoms: #1 -x, y+1/2, -z+1/2, #2 x-1, y, z, #3 -x, y-1/2, -z+1/2, #4 x+1, y, z.

S4. Heterogeneous MO degradation by Co-MOF/PMS

A general pseudo-first-order reaction was used to estimate the degradation reaction rate as shown below:

$$\ln(C/C_0) = -kt$$

where C_0 and C are the initial concentration and the concentration at various time, respectively, k is the first order reaction kinetic constant of MO removal (min^{-1}).

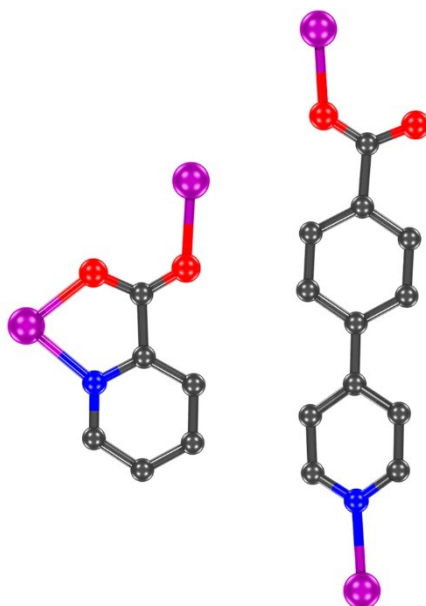


Fig. S1 The coordination modes of ligands in Co-MOF.

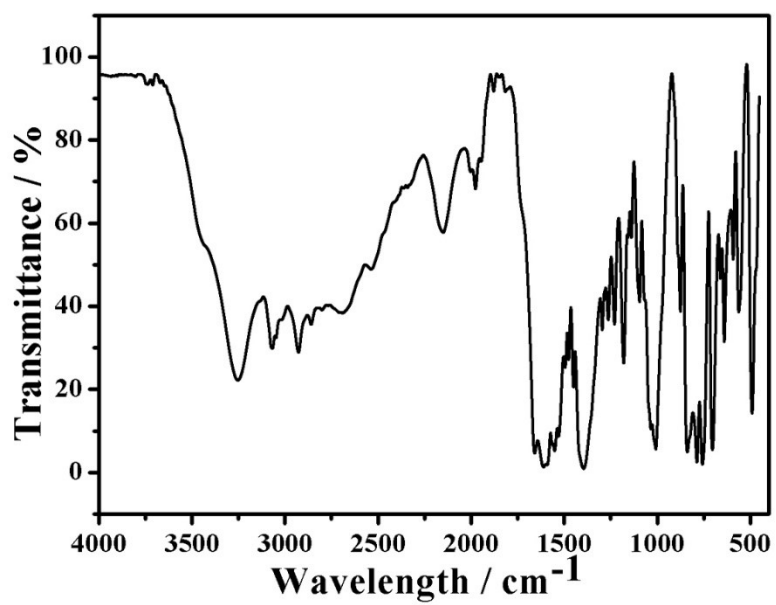


Fig. S2 The FT-IR curve of as-synthesized Co-MOF at room temperature.

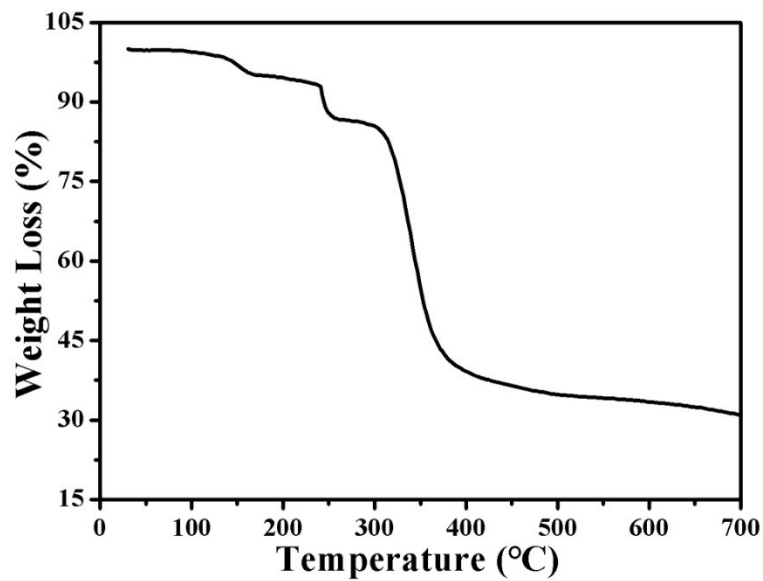


Fig. S3 TGA curve of as-synthesized Co-MOF under nitrogen gas atmosphere.

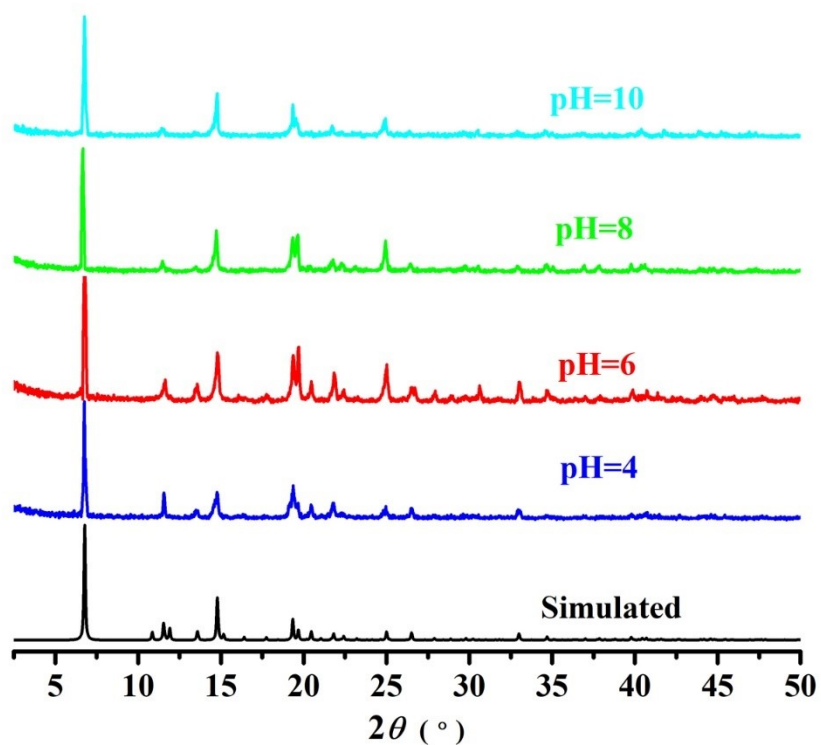


Fig. S4 The PXRD patterns of Co-MOF after immersed in different aqueous solutions with the pH values in the range of 4-10 for 6 h.

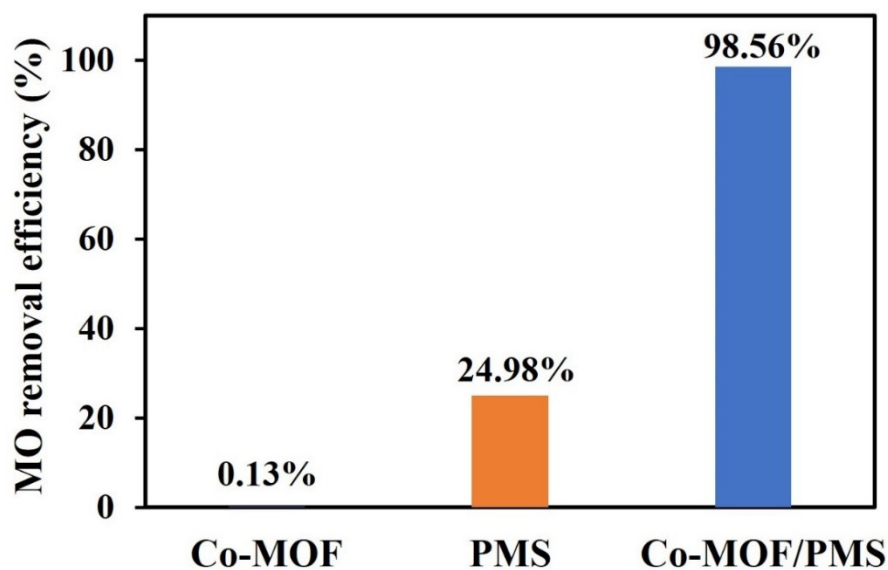


Fig. S5 MO degradation removal efficiency in 5 min under different reaction conditions. [MO] = 20 mg/L, [PMS] = 1.0 mM; [catalyst Co-MOF] = 10 mg; T = 20 °C.

Table S3 Comparison of different Co-containing catalysts towards pollutants for PMS activation.

Catalyst	pollutant	PMS dose	Catalyst dose (g/L)	Degradation efficiency (>95%)	Ref.
HCo ₃ O ₄ /C	BPA, 87.6 μm	325.3 μM	0.1	97%, 4 min	5
Co ₃ O ₄ /N/C	Aniline, 20 ppm	0.15 g/L	0.01	99.4%, 10 min	6
Fe ₃ Co ₇ @C-650	BPA, 20 mg/L	0.2 g/L	0.1	98%, 30 min	7
CoMn ₂ O ₄	SA, 10 mg/L	0.1 g/L	0.05	100%, 30 min	8
Co ₃ O ₄ -palygorskite composites	SMX, 30 μM	0.3 mM	0.125	100%, 3.5 min	9
ZIF-67/PAN	AY, 500 mg/L	0.5 g/L	0.233	95.1%, 10 min	10
Co ₃ O ₄ -MC	OTC, 40 μM	0.5 mM	0.2	100%, 12 min	11
NiCo-LDH/10	RR-120, 0.1 mM	3 mM	0.005	89%, 10 min	12
CuCo-MOF-74	MB, 0.2 mM	2.0 mM	0.05	100%, 30 min	13
Co-BTC	DBP, 0.018 mM	1.62 mM	0.3	90%, 5 min	14
Co-MOF	MO, 20 mg/L	1.0 mM	0.1	98.56%, 4.5 min	this work

BPA, bisphenol A, SA, sulfanilamide, SMX, sulfamethoxazole, AY, acid yellow,

OTC, oxytetracycline, RR-120, Reactive Red-120, DBP, dibutyl phthalate.

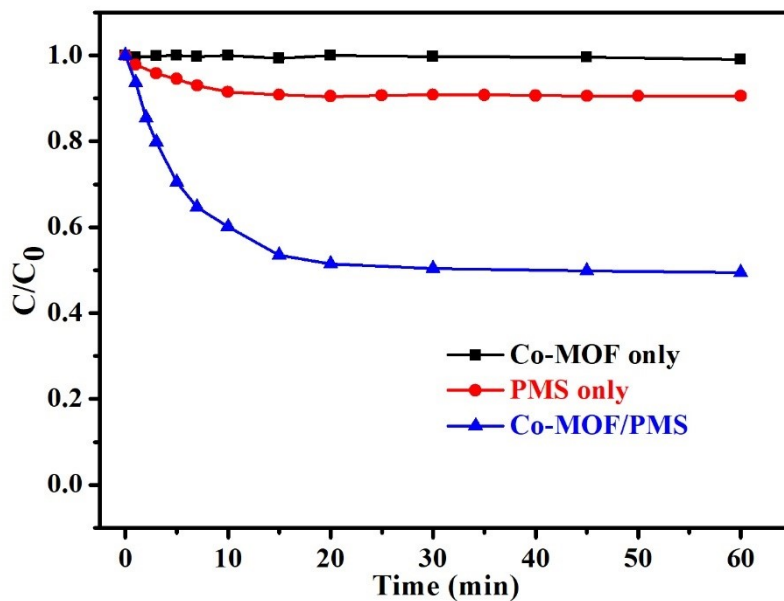


Fig. S6 The bisphenol A degradation efficiency under different reaction systems. [bisphenol A] = 20 mg/L, [PMS] = 1.0 mM; [Co-MOF] = 10 mg; T = 20 °C.

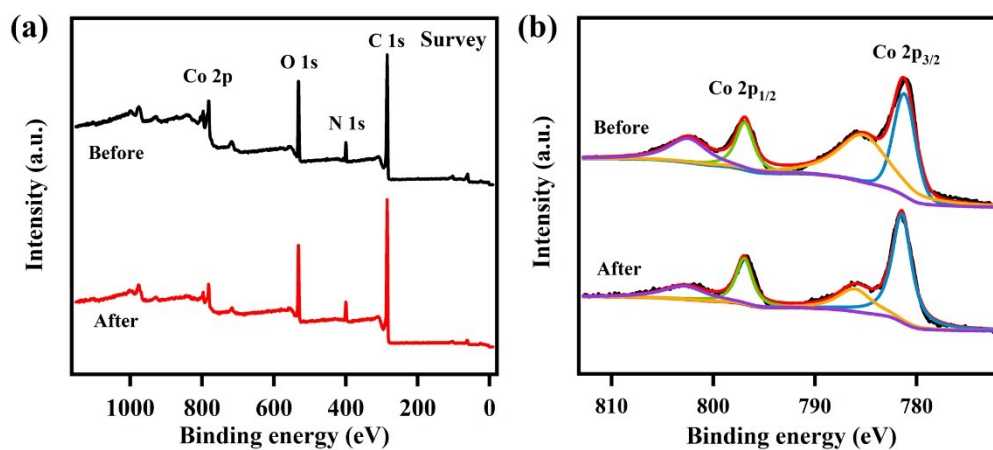


Fig. S7 The XPS spectra of the Co-MOF before and after reaction: (a) survey, and (b) Co 2p.

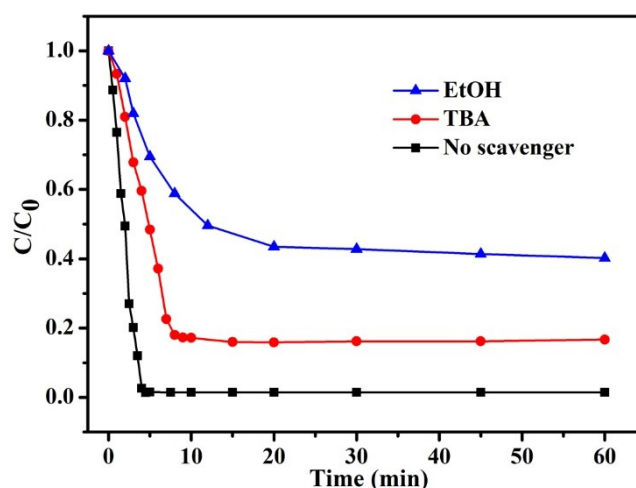


Fig. S8 Radical competition tests for the degradation of MO: quenching agents of EtOH (0.2 M) and TBA (0.2 M). The reaction conditions are based on [MO] = 20 mg/L, [PMS] = 1.0 mM; [catalyst Co-MOF] = 10 mg; T = 20 °C.

References:

1. L. J. Bourhis, O. V. Dolomanov, R. J. Gildea, J. A. K. Howard, H. Puschmann, *Acta Cryst. A.*, 2015, **71**, 59-75.
2. O. V. Dolomanov, L. J. Bourhis, R. J. Gildea, J. A. K. Howard, H. Puschmann, J. *Appl. Crystallogr.*, 2009, **42**, 339-341.
3. G. M. Sheldrick, *Acta Cryst. C.*, 2015, **71**, 3-8.
4. A. Spek, *Acta Cryst. D.*, 2009, **65**, 148-155.
5. M. A. N. Khan, P. K. Klu, C. Wang, W. Zhang, R. Luo, M. Zhang, J. Qi, X. Sun, L. Wang, J. Li, *Chem. Eng. J.*, 2019, **363**, 234-246.
6. Q. Huang, J. Zhang, Z. He, P. Shi, X. Qin, W. Yao, *Chem. Eng. J.*, 2017, **313**, 1088-1098.
7. X. Li, A. I. Rykov, B. Zhang, Y. Zhang, J. Wang, *Catal. Sci. Technol.*, 2016, **6**, 7486-7494.
8. C.-X. Li, C.-B. Chen, J.-Y. Lu, S. Cui, J. Li, H.-Q. Liu, W.-W. Li, F. Zhang, *Chem. Eng. J.*, 2018, **337**, 101-109.
9. Y. Yu, Y. Ji, J. Lu, X. Yin, Q. Zhou, *Chem. Eng. J.*, 2021, **406**, 126759.
10. C. Wang, H. Wang, R. Luo, C. Liu, J. Li, X. Sun, J. Shen, W. Han, L. Wang, *Chem. Eng. J.*, 2017, **330**, 262-271.

11. Z. Li, M. Wang, C. Jin, J. Kang, J. Liu, H. Yang, Y. Zhang, Q. Pu, Y. Zhao, M. You, Z. Wu, *Chem. Eng. J.*, 2020, **392**, 123789.
12. R. Ramachandran, T. Sakthivel, M. Li, H. Shan, Z.-X. Xu, F. Wang, *Chemosphere*, 2021, **271**, 128509.
13. H. Li, Z. Yang, S. Lu, L. Su, C. Wang, J. Huang, J. Zhou, J. Tang, M. Huang, *Chemosphere*, 2021, **273**, 129643.
14. H. Li, J. Wan, Y. Ma, Y. Wang, X. Chen, Z. Guan, *J. Hazard. Mater.*, 2016, **318**, 154-163.